

# Electric field induced anomalies in ferroelectric $K_2SeO_4$

To cite this article: J Leist *et al* 2008 *J. Phys.: Condens. Matter* **20** 415209

View the [article online](#) for updates and enhancements.

## Related content

- [Switching behaviour of modulated ferroelectrics: the kinetics of the field induced lock-in transition in  \$K\_2SeO\_4\$](#)   
J Leist, H Gibhardt, K Hradil *et al.*
- [Switching kinetics of the ferroelectric transition in  \$K\_2SeO\_4\$  studied by stroboscopic gamma-ray diffraction](#)  
J Leist, H Gibhardt and G Eckold
- [Electronic properties and phase transitions in low-dimensional semiconductors](#)  
A M Panich

## Recent citations

- [Direct observation of polar nanodomains in the incommensurate phase of  \$\(K\_{0.96}Rb\_{0.04}\)\_2ZnCl\_4\$  crystals using piezo force microscopy](#)  
Claudia Kofahl *et al*
- [Metastable states and defect density waves in modulated ferroelectrics](#)  
Karsten Behrendt and Götz Eckold
- [The role of defects for the lock-in transition and the formation of polar nanodomains in  \$A\_2BX\_4\$ -compounds](#)  
Karsten Behrendt and Götz Eckold



**IOP | ebooks™**

Bringing together innovative digital publishing with leading authors from the global scientific community.

Start exploring the collection—download the first chapter of every title for free.

# Electric field induced anomalies in ferroelectric $\text{K}_2\text{SeO}_4$

J Leist, H Gibhardt, K Hradil and G Eckold

Institute of Physical Chemistry, University of Göttingen, Germany

Received 23 May 2008, in final form 1 August 2008

Published 16 September 2008

Online at [stacks.iop.org/JPhysCM/20/415209](http://stacks.iop.org/JPhysCM/20/415209)

## Abstract

The lock-in transition of  $\text{K}_2\text{SeO}_4$  at 93.2 K was studied using high-resolution  $\gamma$ -ray diffraction, *in situ* dielectric measurements and neutron scattering. The phase transition shows a coexistence regime of 1.0 K with clearly resolved incommensurate and commensurate satellite reflections. Within a temperature interval of several K above the lock-in transition, strong third order satellites are observed, indicating a pronounced squaring of the modulation wave. Under the influence of high electric fields an intermediate phase is observed, which is characterized by a diffuse intensity distribution. In addition, the dielectric permittivity exhibits two maxima, indicating the existence of two separate phase transitions. This behaviour is attributed to distortions of the discommensuration lattice and pinning of the discommensurations by accumulated charged defects. It seems to be characteristic for modulated ferroelectrics of the  $\text{A}_2\text{BX}_4$  group, since a similar behaviour is also found in isostructural  $\text{Rb}_2\text{ZnCl}_4$  and  $\text{K}_2\text{ZnCl}_4$ . The soft-mode dynamics close to  $T_c$  is found to be essentially independent of the electric field and not affected by the discommensuration lattice.

## 1. Introduction

The family of  $\text{A}_2\text{BX}_4$ -compounds exhibits a rich variety of solid phases including incommensurately modulated and ordered ferroelectric structures. This structural behaviour and the sequence of phase transitions that are observed as a function of temperature is the result of a delicate balance between competing interactions of  $\text{BX}_4$ -tetrahedra and  $\text{A}^+$ -cations. A review of many important properties of this class of materials has been provided by Cummins [1]. While most of the phase transitions leading to incommensurate (INC) phases of these compounds are of the order–disorder type,  $\text{K}_2\text{SeO}_4$  provides a special example of a displacive transition induced by a soft phonon mode [2]. On cooling from the ambient-temperature paraelectric orthorhombic phase (space group  $Pm\bar{c}n$ )<sup>1</sup>, the condensation of an optical soft mode at  $T_i = 126.7$  K leads to an INC-phase. This is characterized by satellite reflections with a modulation wavevector  $\mathbf{q} = (2/3 + \delta)\mathbf{c}^*$  and a temperature dependent misfit parameter  $\delta$ . At  $T_c = 93.2$  K, the modulation locks to a commensurate value through a discontinuous vanishing of the misfit parameter. The commensurate (C) phase has a tripled unit cell and the space group  $P2_1cn$ . It is an improper ferroelectric with a spontaneous polarization along the  $a$ -direction.

<sup>1</sup> Note that our setting corresponds to the following lattice parameters at room temperature:  $a = 6.003$  Å,  $b = 10.455$  Å,  $c = 7.661$  Å.

The dynamics of the incommensurate phase is usually discussed in terms of phason and amplitudon modes as new elementary excitations in addition to the ordinary phonon modes [3, 4]. While a good number of investigations have been focused on the temperature dependence of vibrational spectra [2–6] and dielectric permittivity [7, 8], little is known about the influence of the electric field on the phase transitions in  $\text{K}_2\text{SeO}_4$ . In other systems like thiourea [9], BCCD [10] etc, new field induced commensurate phases have been detected. Such a behaviour is absent in  $\text{Rb}_2\text{ZnCl}_4$  and  $\text{K}_2\text{SeO}_4$  being prominent representatives of  $\text{A}_2\text{BX}_4$  compounds. This demonstrates that the response to an applied electric field crucially depends on the structural properties of the system under consideration. It is generally accepted that the ferroelectric commensurate C-phase is stabilized by the application of an external electric field  $E$  along the polar axis  $\mathbf{a}$ . Consequently, the temperature of the lock-in transition increases with  $E$ . This simple behaviour is frequently observed in modulated ferroelectrics like  $[\text{N}(\text{CH}_3)_4]_2\text{ZnCl}_4$  [11] and also in earlier investigations of  $\text{Rb}_2\text{ZnCl}_4$  and  $\text{K}_2\text{SeO}_4$  [12]. In  $(\text{NH}_4)_2\text{BeF}_4$  [13] and  $\text{Rb}_2\text{ZnBr}_4$  [14], however, a more complicated behaviour is found and field induced intermediate phases between the INC- and the C-phases are reported. A recent high-resolution investigation of purified  $\text{Rb}_2\text{ZnCl}_4$  using  $\gamma$ -ray diffraction revealed that such a phase is present even in this well studied compound [15]. The diffraction pattern

of this phase is characterized by a broad diffuse intensity distribution instead of well defined satellite reflections. With the present study we want to demonstrate that different from the findings of Fousek *et al* [12] such a behaviour is also present in the soft-mode-driven system  $\text{K}_2\text{SeO}_4$ . Hence, it might be regarded as a common feature of modulated  $\text{A}_2\text{BX}_4$ -compounds.

Before we are going to discuss the experimental findings, let us briefly recall the commonly accepted mechanism of lock-in transitions in dielectrics: on cooling below  $T_i$ , the modulated structure of the INC-phase is described by a sinusoidal plane wave. Approaching the lock-in transition at  $T_c$ , the modulation wave becomes increasingly distorted. Close to  $T_c$ , the INC-phase consists of an ordered arrangement of commensurate nanodomains that differ only by the phase of the order parameter. In the case of  $\text{K}_2\text{SeO}_4$ , there are six different domains according to the threefold superstructure of the C-phase. These domains are separated by boundaries perpendicular to the modulation wavevector called discommensurations (DCs) [16] where the phase of the order parameter changes by  $\Delta\phi = \pi/3$ . The DC-density is directly related to the misfit parameter  $\delta$  and, hence, it changes continuously with temperature. It was demonstrated by Janovec [17] and Kawasaki [18] that the creation or annihilation of discommensurations requires the nucleation and growth of topological defects, so-called stripples and antistripples, that consist of a whole sequence of six domains. This stripple mechanism was in detail studied by molecular-dynamics simulations by Parlinski *et al* [19–21] and the defects could, in fact, be directly observed by transmission electron microscopy by Sakata *et al* [22]. Moreover, in  $\text{Rb}_2\text{ZnCl}_4$  a detailed structure determination of the incommensurate phase has been performed recently by Aramburu *et al* [23], based on intensities of satellite reflections of first and higher orders in a variety of Brillouin zones. Various nuclear magnetic resonance (NMR) investigations of several  $\text{A}_2\text{BX}_4$ -compounds have been reported that allow to determine not only the critical behaviour of the order parameter and the soliton density [24–26] but also the different dynamical properties of nuclei located within the commensurate domains and the discommensurations, respectively [27–30].

In  $\text{K}_2\text{SeO}_4$ , each DC separates two ferroelectric domains of opposite polarization. Therefore, the density and the mobility of DCs essentially determine the dielectric permittivity. Since close to  $T_c$ , the misfit parameter  $\delta$  and, consequently, the DC-density become rather small, even few defects are able to pin the DCs and hinder the lock-in transition.

High-resolution  $\gamma$ -ray diffraction is an extremely powerful tool to study the real structure of crystals and to determine the positions and widths of satellite reflections with high accuracy. Hence, it is possible to determine even tiny changes in the DC-density during the lock-in transition that provides detailed information about the underlying microscopic mechanism. In the present study, the influence of applied electric fields on the modulated structure was studied within the temperature-range of the lock-in transition.

## 2. Experimental details

Large single crystals of  $\text{K}_2\text{SeO}_4$  were grown from aqueous solution by slow evaporation. The starting material was carefully purified using fractionated crystallization as well as extraction of the solution to reduce substitutional defects like sodium, e.g. Hence, high quality crystals were obtained with mosaicities less than  $0.03^\circ$ . Due to the almost hexagonal metric of the unit cell ( $b \approx \sqrt{3}a$ ), twinning is commonly encountered in  $\text{K}_2\text{SeO}_4$ . With the help of polarization microscopy, monodomain samples with sizes of about  $2 \times 5 \times 5 \text{ mm}^3$  could be prepared. The correct assignment of the crystal axes was confirmed by careful determination of the angle between the (2 0 0) and (1 3 0) reflections. For the application of electric fields up to  $10 \text{ kV cm}^{-1}$ , electrodes were applied to the a-faces of the sample with silver paint. The samples were mounted in a closed-cycle cryostat allowing for a temperature stability of better than 0.05 K. The actual sample temperature was determined by a platinum resistor mounted close to the sample position.

High-resolution  $\gamma$ -diffraction patterns were obtained in the  $\omega$ -scan technique using 316 keV  $\gamma$ -rays from an  $^{192}\text{Ir}$  source. Most of the satellite spectra were taken close to (2 0 2/3) or (2 0 4/3) superlattice reflections. High-energy resolution and tight collimation yields a transverse resolution of about  $10^{-3} \text{ \AA}^{-1}$ . *In situ* impedance spectroscopy allowed us to determine the dielectric permittivity  $\varepsilon$  of the sample simultaneously. Note, that influences of radiation damage can definitely be ruled out due to the limited flux of the  $\gamma$ -source ( $\approx 10^7 \text{ cm}^{-2} \text{ s}^{-1}$ ) corresponding to a dose rate of less than 0.02 Gy per day.

Neutron scattering experiments on higher order satellites as well as on the soft phonon have been performed at the triple axis spectrometer PUMA at FRM II in Garching. Higher order satellite reflections were recorded using a wavelength of  $2.36 \text{ \AA}$  along with a filter of pyrolytic graphite. The beam was tightly collimated with a divergence of  $0.25^\circ$  before and after the sample. For the phonon investigations the high-intensity double focusing mode of the PUMA spectrometer was used.

## 3. Results

### 3.1. Detailed characterization of the lock-in transition in zero field

The lock-in transition is best characterized by the behaviour of satellite reflections. The temperature dependence of the satellite positions at zero electric field is shown in figure 1. The wavevector of the INC-satellite decreases as the sample is cooled. At 93.2 K, the appearance of the C-satellite at exactly  $\mathbf{q} = 2/3\mathbf{c}^*$  indicates the onset of the lock-in transition. Over a temperature interval of 1.0 K both the INC- and C-satellites do coexist, a behaviour that is frequently observed in modulated systems. A typical diffraction pattern of this coexistence regime is shown as an inset in figure 1. It can be seen that both satellites are well separated due to the high resolution of the  $\gamma$ -diffractometer. Note, that the width of the INC-satellite increases gradually by almost 70% during the

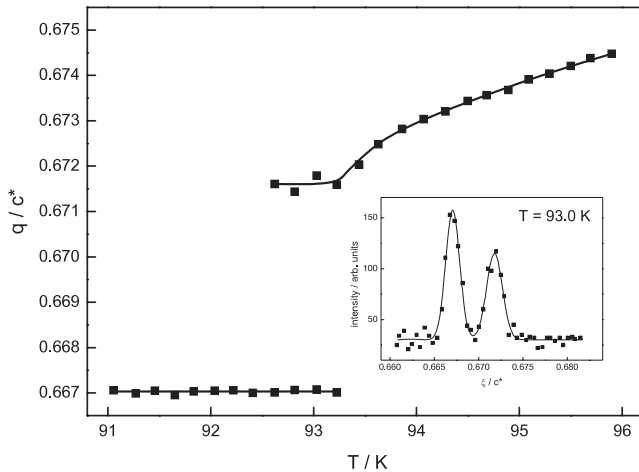


**Figure 1.** Temperature dependence of the  $(2\ 0\ 2/3 + \delta)$ -satellite position at zero field on cooling. The inset shows a typical intensity profile taken within the coexistence regime at 93.0 K.

transition while its position remains constant. The C-satellite, on the other hand, appears only slightly broader within the coexistence regime than well below the phase transition where its FWHM corresponds to that of fundamental reflections like  $(2\ 0\ 0)$ .

The broadening of the INC-satellite and the coexistence regime is definitely not due to thermal gradients. The upper limit of a possible temperature gradient across the sample can be estimated by comparing the widths of the INC- and C-satellites well above and below the lock-in transition. It is found that between 96 and 94 K the INC-satellite is broader than the commensurate one below the transition by about  $1.5 \times 10^{-4} c^*$ , only. Since its centre position changes by  $8 \times 10^{-4} c^* K^{-1}$  in this temperature interval, it can be inferred that a possible gradient cannot be larger than 0.2 K. Hence, we conclude that the broadening of the INC-satellite during the lock-in transition is caused by those defects that are able to pin the discommensurations and reduce the coherence of the modulation wave.

Within the coexistence regime, the wavevector of the INC-satellite remains constant corresponding to the minimum misfit parameter of  $\delta = 4.6 \times 10^{-3}$  in good agreement with lower resolution x-ray studies [31, 32]. This finding may not be confused with the appearance of well defined steps in the temperature variation of  $\delta$  which is characteristic for devil's staircase systems like BCCD and others [10]. Here, it is a signature of the phase coexistence rather than a separate lock-in phase. A possible description in terms of a commensurate superstructure would demand a non-physically large unit cell. Hence, we conclude that the actual structure is described by a regular arrangement of discommensurations.

The density of discommensurations as obtained by

$$\rho_{DC} = \frac{6\delta}{c} \quad (1)$$

is evaluated as  $0.036\text{ nm}^{-1}$  and corresponds to the distance between adjacent DCs of about 36 lattice constants (28 nm). This value is about three times larger than that found in the

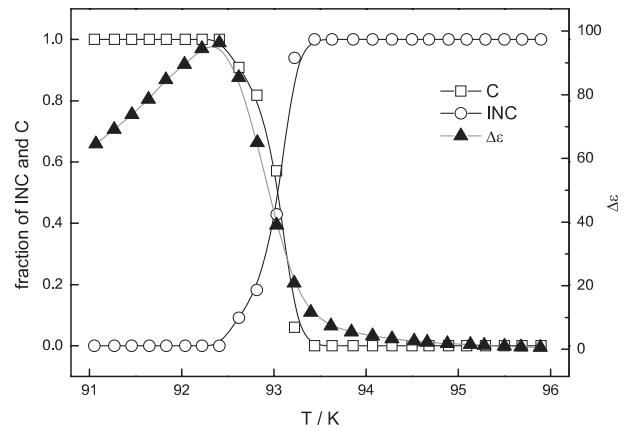


**Figure 2.** Temperature dependence of the volume fractions of both modulated phases and dielectric permittivity (at 1 kHz) on cooling.

isostructural  $Rb_2ZnCl_4$ , reflecting the fact that the attractive interaction between adjacent DCs is considerably weaker in  $K_2SeO_4$ . The discontinuous behaviour of the modulation wavevector clearly proves the first order nature of the lock-in transition.

The rather small discommensuration density within the INC-phase is most probably the reason why in  $K_2SeO_4$ , the C-phase is almost free from residual DCs and the satellite reflection is detected just at the ideal  $2/3$ -position. This is in contrast to the findings in  $Rb_2ZnCl_4$  where a small but significant deviation was reported at the onset of the phase transition and attributed to the existence of some residual DCs [33]. From NMR-experiments, Topic *et al* [26] have determined the volume fraction of discommensurations (in their paper called ‘soliton density’) and found the existence of a good number of DCs in  $K_2SeO_4$  even below  $T_c$ . As stated by the authors, this effect depends on the number of defects present in the crystal. It is commonly accepted that the size of the thermal hysteresis is directly related to the sample quality [34]. In our sample, the hysteresis of the lock-in transition is as small as 0.2 K due to the substantial effort in the purification process prior to crystal growth. Hence, we attribute the considerably smaller number of residual DCs to the high quality of our sample.

The lock-in transition is associated with a pronounced maximum of the (real part of the) dielectric permittivity just as observed already by Aiki *et al* [7]. Its temperature dependent contribution,  $\Delta\epsilon$ , is displayed in figure 2 along with the volume fractions of the INC- and C-phases as determined from the integrated intensities of the respective satellite reflections. Interestingly, the maximum of  $\Delta\epsilon$  is found at the lowest temperature of the coexistence regime, just when the INC-phase is going to disappear completely.

Note, that similar to the observations in other ferroelectric modulated systems [35, 36], the dielectric permittivity exhibits a long-term relaxation after a change in temperature with time constants of several minutes. Obviously, the nucleation of antistriplets and the subsequent relaxation of the remaining DCs needs quite a long time. Even if the crystal is rather perfect, a small number of remaining defects is sufficient to act

as pinning centres owing to the small DC-density. Since the recording of satellite spectra usually takes more than an hour this relaxation process is not visible with  $\gamma$ -ray diffraction.

Within the commensurate phase, the dielectric permittivity exhibits a broad tail in its temperature dependence in very good agreement with the findings of Aiki *et al* [7] and Horioka *et al* [8]. This is usually attributed to some residual discommensurations [37]. From the diffraction data, however, we have concluded, that the corresponding density must be extremely small. Hence, the anomalous behaviour of  $\Delta\epsilon$  indicates that these few DCs, that are just ordinary domain walls within the C-phase, exhibit a rather large mobility.

### 3.2. Higher order satellites, squaring and the soliton regime

The appearance of higher order satellites provides information about the deviation of the structural modulation from a simple sinusoidal plane wave. We have restricted ourselves to the study of the third order satellite  $(2\ 0\ 3\delta)$ . Due to intensity reasons, we could not detect this reflection with  $\gamma$ -rays. Neutrons, on the other hand, yield intensities that are only about a factor of 40 smaller than those of the strongest first order satellites and far larger than other higher harmonics. Figure 3 shows the temperature dependence of the normalized intensities of  $(2\ 0\ 4/3 - \delta)$  and the  $(2\ 0\ 3\delta)$  satellites as determined with the three axes spectrometer PUMA. The intensity of the first order satellite can well be described by a power law with an exponent  $2\beta = 0.56 \pm 0.01$  within the entire temperature regime of the incommensurate phase, except the close vicinity of  $T_i$ . Since we concentrated on the field and temperature dependence of satellites close to the lock-in transition, no attempt has been made to study the critical behaviour near  $T_i$ . This has already been done by Majkrzak *et al* [38] who found a critical exponent of about  $2\beta = 0.75$  within the temperature regime of 10 K below  $T_i$ . This value is in close agreement with the prediction from renormalization group theory for the universality class of the 3d-XY model ( $2\beta = 0.692$ ) [39] to which  $\text{K}_2\text{SeO}_4$  belongs [40]. The same critical behaviour has been confirmed by NMR-techniques [41] in other compounds of the  $\text{A}_2\text{BX}_4$ -family. In some cases, the power law holds from  $T_i$  down to the lock-in transition at  $T_c$ . In  $\text{K}_2\text{SeO}_4$ , however, our results (figure 3) show that on cooling below about 115 K, the temperature dependence of the first order satellite intensity is considerably weaker than expected from the critical behaviour (dotted line). Interestingly, this is just that temperature regime where the third order satellite starts to grow dramatically on approaching  $T_c$  as illustrated in figure 3.

The third order satellite is particularly sensitive to the squaring of the modulation wave and, as a consequence, also on the discommensuration pattern or soliton density, as will be shown in the following.

The structure factor is usually described by the displacements  $\mathbf{u}_{kl}$  of all atoms  $k$  within the unit cell  $l$ :

$$F(\mathbf{Q}) = \sum_l \sum_k b_k \exp(i\mathbf{Q}(\mathbf{r}_k^0 + \mathbf{r}_l + \mathbf{u}_{kl})) \quad (2)$$

$\mathbf{r}_k^0 + \mathbf{r}_l$  being the equilibrium position of the atom  $(kl)$  in the non-modulated structure, and  $b_k$  the scattering length.

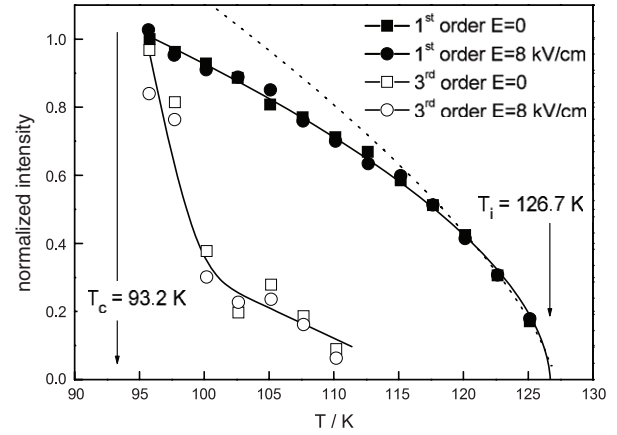


**Figure 3.** Normalized integrated intensities of the first and third order satellites,  $(2\ 0\ 4/3 - \delta)$  and  $(2\ 0\ 3\delta)$ , respectively. The line through the first order data is the result of a fit by a power law while the line through the third order data is a guide to the eye only. The dotted line corresponds to the critical behaviour with the exponent  $2\beta = 0.692$  close to  $T_i$  according to the prediction for the 3d-XY model [39].

The displacement is described by a plane wave of wavevector  $\mathbf{q}$  and polarization vectors  $\mathbf{e}_k$ ,

$$\mathbf{u}_{kl} = \mathbf{e}_k \exp(i\mathbf{q}\mathbf{r}_l). \quad (3)$$

Non-sinusoidal modulation waves give rise to higher harmonics:

$$\mathbf{u}_{kl} = \sum_m \mathbf{e}_k^{(m)} \exp(im\mathbf{q}\mathbf{r}_l). \quad (4)$$

For small displacements, the exponential in equation (2) may be expanded in a Taylor series to yield:

$$\begin{aligned} F(\mathbf{Q}) &= \sum_l \sum_k b_k \exp(i\mathbf{Q}(\mathbf{r}_k^0 + \mathbf{r}_l)) \sum_{n=0}^{\infty} \frac{1}{n!} (i\mathbf{Q}\mathbf{u}_{kl})^n \\ &= \sum_l \sum_k b_k \exp(i\mathbf{Q}(\mathbf{r}_k^0 + \mathbf{r}_l)) \\ &\quad \times \sum_{n=0}^{\infty} \frac{1}{n!} \left( i\mathbf{Q} \sum_{m=1}^{\infty} \mathbf{e}_k^{(m)} \exp(im\mathbf{q}\mathbf{r}_l) \right)^n \\ &= \sum_k b_k \exp(i\mathbf{Q}\mathbf{r}_k^0) \sum_{n=0}^{\infty} \frac{(i)^n}{n!} \\ &\quad \times \sum_{m_1=1}^{\infty} \mathbf{Q}\mathbf{e}_k^{(m_1)} \sum_{m_2=1}^{\infty} \mathbf{Q}\mathbf{e}_k^{(m_2)} \cdots \sum_{m_n=1}^{\infty} \mathbf{Q}\mathbf{e}_k^{(m_n)} \\ &\quad \times \sum_l \exp[i(\mathbf{Q} + (m_1 + m_2 + \cdots + m_n)\mathbf{q}) \cdot \mathbf{r}_l]. \end{aligned} \quad (5)$$

Hence, for an infinite crystal, satellite reflections are expected at

$$\mathbf{Q} = \mathbf{g} - (m_1 + m_2 + \cdots + m_n)\mathbf{q}, \quad m_i, n = 1 \cdots \infty \quad (6)$$

$\mathbf{g}$  being a reciprocal lattice vector of the parent lattice.

As already pointed out by Parlinski [21], there are two types of satellites characterized by the indices  $m_i$  and  $n$ , respectively. Harmonics corresponding to  $m_i = 1$  are called ‘diffraction harmonics’ with wavevectors  $n\mathbf{q}$ . Satellites resulting from a squaring of the modulation are

frequently observed and predicted by molecular-dynamics simulations [21]. These are called ‘distortion harmonics’ characterized by  $m_i = 3, 5, 7, \dots$

Frequently, the displacement  $\mathbf{u}_{kl}$  is represented by a sinusoidal commensurate wave with periodic phase shifts (discommensurations):

$$\mathbf{u}_{kl} = \mathbf{e}_{kl} \exp \left( i \left( \mathbf{q}_c \mathbf{r}_l + \sum_{r=1}^{\infty} c_r \sin(pr \mathbf{q}_c \mathbf{r}) \right) \right) \quad (7)$$

with  $p = 6$  in the case of threefold commensurate superstructures. It has been shown by Aslanyan [42], Aramburu [23] and others that in this case higher order satellites are expected only at

$$\mathbf{Q} = \mathbf{g} - (6r \pm 1)\mathbf{q}, \quad r = 0 \dots \infty \quad (8)$$

$\mathbf{q}$  being the effective incommensurate wavevector

$$\mathbf{q} = \mathbf{q}_c - \frac{\delta}{3} \mathbf{c}^*. \quad (9)$$

Consequently, the strong third order satellites observed in  $\text{K}_2\text{SeO}_4$  and previously also in  $\text{Rb}_2\text{ZnCl}_4$  [33] cannot be explained on the basis of the usual structure determination procedure. Rather, as has been pointed out already by Pérez-Mato *et al* [43], the interaction of different modes of modulation is responsible for this type of satellites. The same coupling leads to the existence of the Lifshitz invariant in the free energy expansion [44]. Hence, the assumption of a sinusoidal commensurate wave with a periodic arrangement of discommensurations (solitons) is not justified in these systems. Rather, the displacement pattern shows considerable squaring effects that are quantitatively characterized by the intensity of third order satellites, in particular.

If, however, as a limiting case, the modulation is described by a true square wave with an incommensurate wavevector  $\mathbf{q}$ , the same displacement pattern of the individual atoms can be described equally well by a squared commensurate wave ( $\mathbf{q}_c$ ) with a periodic arrangement of discommensurations. This is illustrated in figure 4 for the simple case with one atom per unit cell. Alternatively, the displacement can also be regarded as a normal-mode amplitude. Part (a) shows a simple sinusoidal with an incommensurate wavevector. The corresponding satellite spectrum consists of first order satellites and weak ‘diffraction harmonics’ ( $n = 1, 2, 3, \dots$ ) only. In part (b) the modulation consists of piecewise sinusoidal regions with commensurate wavevector, separated by discommensurations, giving rise to higher order harmonics of the type described by equation (8). A commensurate square wave with discommensurations and a square wave with incommensurate wavevector are illustrated in parts (c) and (d), respectively. Both descriptions are entirely equivalent as long as the actual displacements of the discrete atoms are considered. The Fourier spectrum exhibits rather strong third order satellites and considerably weaker other higher order components, just as observed in  $\text{K}_2\text{SeO}_4$  and  $\text{Rb}_2\text{ZnCl}_4$ . Hence, the existence of the third order satellite in  $\text{K}_2\text{SeO}_4$  is directly associated with the squaring of the modulation

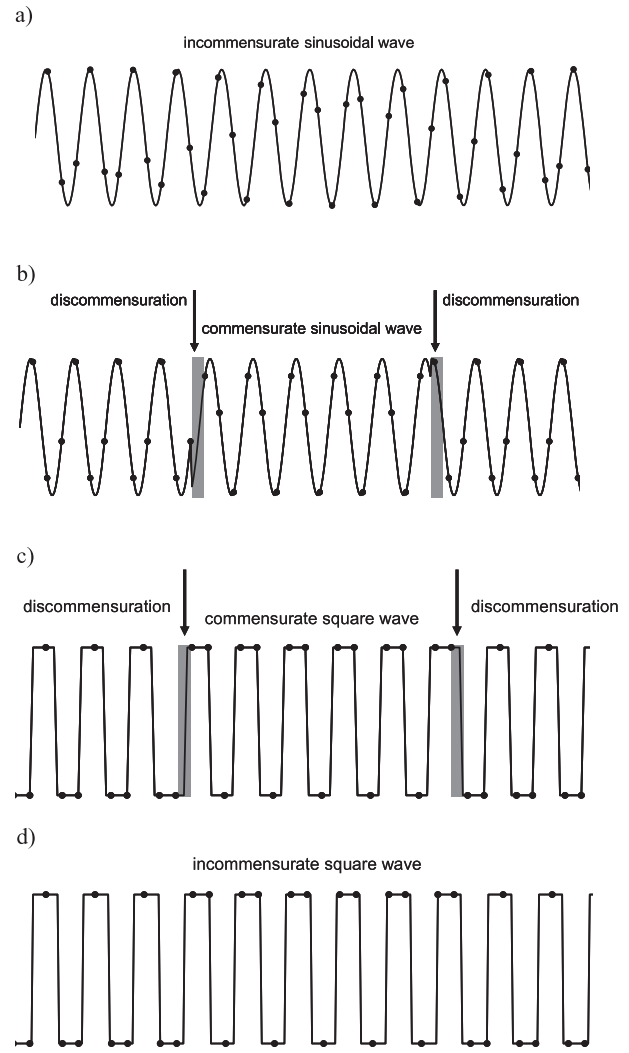


**Figure 4.** Comparison of modulation patterns with the positions of individual atoms; (a) incommensurate sinusoidal wave, (b) commensurate sinusoidal wave with discommensurations, (c) commensurate square wave with discommensurations, (d) incommensurate square wave.

wave and, as a consequence, also with the existence of a discommensuration or soliton lattice.

From the data shown in figure 3, we therefore conclude that in  $\text{K}_2\text{SeO}_4$ , squaring is particularly important in a temperature interval of several K above the lock-in transition. Hence, at least in this temperature regime, the modulation can well be described by a soliton lattice separating domains with antiparallel polarization. This view is supported by NMR-results from isostructural  $\text{Rb}_2\text{ZnCl}_4$  [27, 28] that show that two kinds of nuclei can clearly be distinguished, those within the discommensurations and those within the commensurate domains.

### 3.3. Applied field dependence of satellite spectra and dielectric permittivity

The influence of an applied electric field on the modulated structure is particularly pronounced close to the lock-in

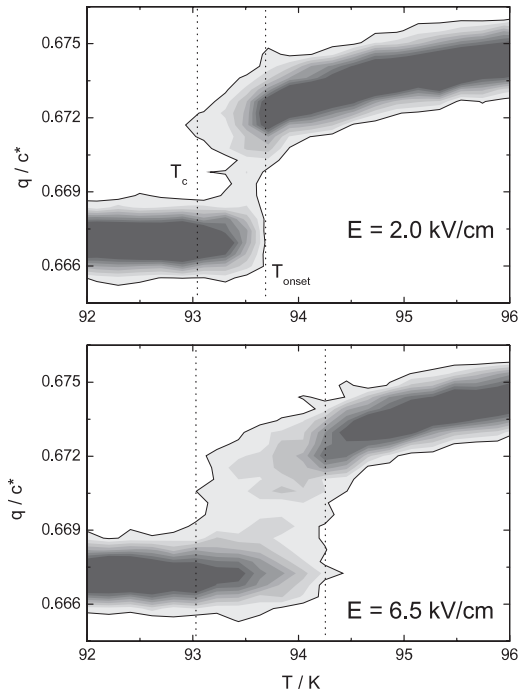


**Figure 5.** Temperature dependence of satellite spectra for two different applied electric fields represented as an iso-intensity contour plot.

transition at  $T_c$ . In figure 5, the temperature dependence of satellite spectra is represented by contour plots for two different applied fields. It is readily seen that the onset of the lock-in transition at  $T_{\text{onset}}$  is shifted to higher temperatures with increasing field as expected from theoretical considerations in the framework of the Landau theory [12]. The temperature  $T_c$  at which the crystal becomes entirely commensurate, however, is hardly changed as shown by the vertical lines in figure 5. Moreover, between  $T_{\text{onset}}$  and  $T_c$ , the diffraction pattern cannot be represented by the superposition of two well defined satellites if the applied field is increased to several  $\text{kV cm}^{-1}$ . Instead, it is characterized by a sharp commensurate satellite and a broad diffuse intensity distribution.

Characteristic satellite profiles at 93.5 and 94 K are shown in figure 6 for an applied field of  $6.5 \text{ kV cm}^{-1}$ . It is clearly seen that at 94.0 K, the spectrum is still dominated by two rather well defined components: a commensurate peak at  $\mathbf{q} = 2/3\mathbf{c}^*$  and a much broader band centred at  $\mathbf{q} \approx 0.672\mathbf{c}^*$ . Comparison with the  $E = 0$  data shown in figure 1 yields that the incommensurate component has become significantly broader. This effect is even more pronounced if the temperature is decreased by 0.5 K (upper part of figure 6). In order to obtain a quantitative description of the experimental data, we tentatively fit both components by Gaussians. Assuming that the volume fractions of the corresponding phases are again given by the respective integrated intensities, we find a behaviour as displayed in figure 7. In the same plot, the temperature dependence of the dielectric permittivity is shown that was measured *in situ* during the diffraction experiments. At weak applied fields, there is a single peak, but now at the onset-temperature of the lock-in transition. In agreement

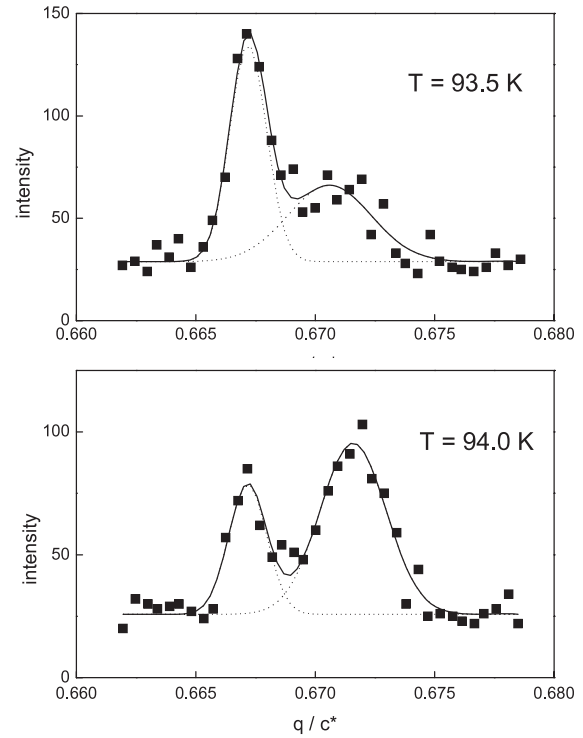


**Figure 6.** Satellite spectra at 93.5 and 94 K under a field of  $6.5 \text{ kV cm}^{-1}$ .

with previous theoretical [45] and experimental studies [7], this peak shifts to higher temperatures as the field strength is increased. At the same time, the maximum value of  $\Delta\varepsilon$  decreases. Within the pure INC-phase, there is almost no field dependence of the permittivity. On increasing the field to values well above  $4 \text{ kV cm}^{-1}$ , however, a second peak is clearly resolved at just that temperature where the lock-in transition is completed. At  $2 \text{ kV cm}^{-1}$  (upper part of figure 7), this second contribution is hidden below the much larger main peak and cannot be clearly resolved. There is, however, an indication of a weak shoulder at about 93 K. Hence, diffraction and dielectric data indicate a two-step transition: in a first step at  $T_{\text{onset}}$ , the INC-phase is transformed into an intermediate phase, and only a second step at  $T_c$  leads from this intermediate phase to the completely ordered commensurate one. The broad satellite pattern within the intermediate phase indicates a strongly reduced coherence length of the modulated structure.

In figure 8, the temperature dependence of the width of the broad component is displayed along with its position for  $E = 6.5 \text{ kV cm}^{-1}$ . For comparison, the corresponding data of the INC-satellite at zero field are also shown. Since the satellite width well above the phase transition corresponds to the instrumental resolution  $\Delta q_{\text{res}}$ , the coherence length may be estimated as

$$\eta = \frac{2\pi}{\sqrt{\Delta q^2 - \Delta q_{\text{res}}^2}}. \quad (10)$$

This yields a value of about 130 nm at  $E = 6.5 \text{ kV cm}^{-1}$  and 93.2 K which corresponds only to about three commensurate domains and is thus considerably smaller than the size of a complete stripple. Hence, it is likely that the

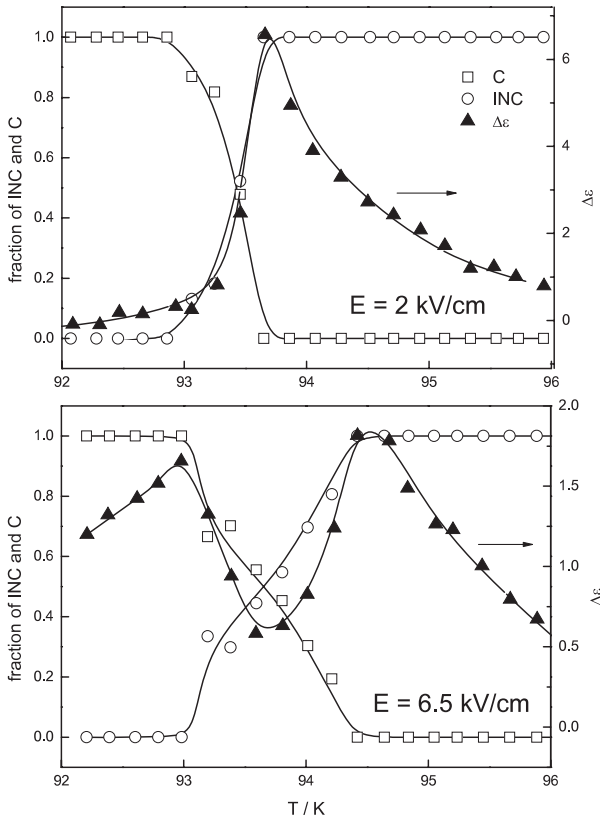


**Figure 7.** Temperature dependence of the dielectric permittivity ( $\blacktriangle$ ) and the volume fractions of the C-phase ( $\square$ ) and the intermediate phase ( $\circ$ ) for  $E = 2 \text{ kV cm}^{-1}$  (top) and  $E = 6.5 \text{ kV cm}^{-1}$  (bottom).

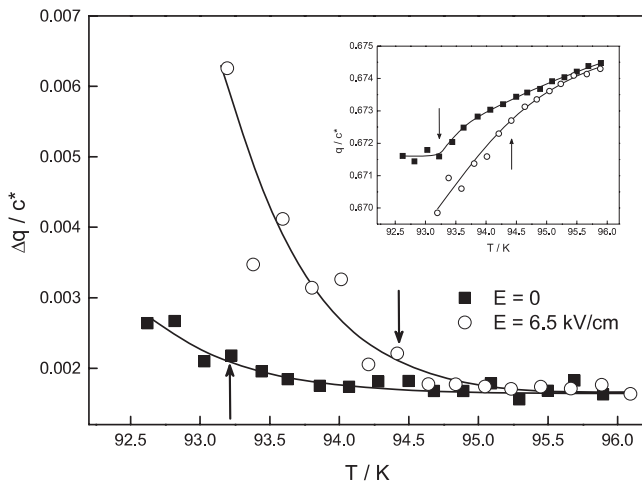


**Figure 8.** Influence of the electric field on the satellite width  $\Delta q$ . Arrows indicate the onset of the phase transition. The inset shows the temperature dependence of the maximum position.

stabilization of the intermediate phase is due to the inability to form antistriplines from pinned discommensurations. As shown in the inset of figure 8, the average wavevector is significantly smaller under the influence of the electric field even above the phase transition.

In the isostructural compound  $\text{Rb}_2\text{ZnCl}_4$ , a similar intermediate phase has been detected recently [15]. In this

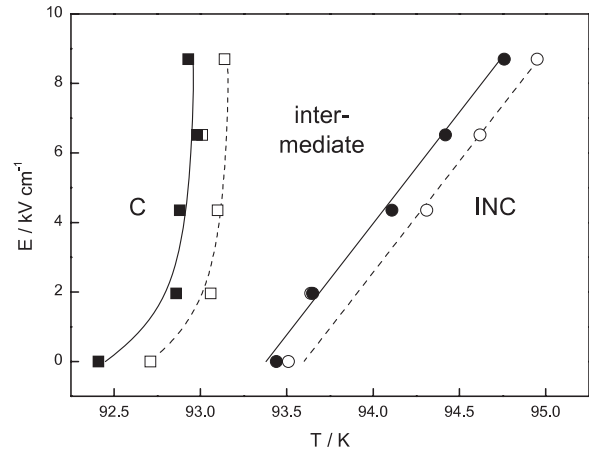


**Figure 9.**  $E-T$  phase diagram. Solid and open symbols represent the transition temperatures on cooling and on heating, respectively.

latter compound, however, no well defined commensurate satellite is observed within the intermediate temperature regime. Rather, the domain structure is completely disordered giving rise to a broad and unstructured intensity distribution. Most probably, the considerably larger DC-density in  $\text{Rb}_2\text{ZnCl}_4$  close to the lock-in transition is responsible for this different behaviour. Indications for a field induced two-step transition have also been obtained from dielectric experiments on  $(\text{NH}_4)_2\text{BeF}_4$  by Strukov *et al* [13], and  $\text{Rb}_2\text{ZnBr}_4$  by Kroupa *et al* [14]. These authors interpret their results on the basis of defect density waves. Structural information is, however, not available in these systems. In  $[\text{N}(\text{CH}_3)_4]_2\text{ZnCl}_4$ , on the other hand, diffraction experiments by Kobayashi *et al* [46] show an increased coexistence regime at  $20 \text{ kV cm}^{-1}$  but no broadening of the satellites.

It should be added that in  $\text{K}_2\text{SeO}_4$ , the two-peak behaviour of the dielectric permittivity has never been observed before. The reason is that all experiments reported in the literature were done on cooling with a constant temperature rate. We have proven that under those conditions, the second peak at lower temperature is definitely absent. In contrast, our *in situ* experiments were performed under quasi-equilibrium conditions, i.e. the sample was held at each temperature for about 90 min—long enough to account for the long-term relaxation effect. Hence, we believe that the present findings are closer to the true equilibrium behaviour of these modulated systems.

### 3.4. The $E-T$ phase diagram

The  $E-T$  phase diagram shown in figure 9 is constructed from the transition temperatures  $T_{\text{onset}}$  and  $T_c$  extracted from diffraction and dielectric data. The phase boundary between the INC and intermediate phase is linear, with a slope  $dT_{\text{onset}}/dE = (0.156 \pm 0.006) \text{ K kV}^{-1} \text{ cm}^{-1}$ . This is slightly smaller than the values reported from earlier dielectric experiments [7, 12]. The lower phase boundary, between the intermediate and the C-phase, is almost independent of the electric field, except for the shift between  $E = 0$  and  $2.0 \text{ kV cm}^{-1}$ . The thermal hysteresis is not affected by the electric field.

### 3.5. Lattice dynamics

In figure 10, the inelastic neutron scattering spectra of the soft phase mode are displayed for some temperatures within the INC-phase and  $\mathbf{Q} = (4\ 0\ 1.2)$ . While previous measurements of Quilichini *et al* [47] had been restricted to temperatures near  $T_i$  and below  $T_c$ , we were able to observe the phase mode throughout the INC-phase and also close to the lock-in transition. On cooling, the quasi-harmonic frequency remains almost constant at 0.4 THz but the line width  $\Delta\nu$  decreases continuously as shown in the inset of figure 10. As soon as the squaring regime is reached, however, the slope becomes considerably smaller. Taking into account the experimental resolution of 0.09 THz we determine a damping constant of about 0.2 THz at  $T_c$  in very good agreement with the findings of Raman-experiments [6]. In contrast to the suggestions of Quilichini [47], the phason damping exhibits a pronounced non-linear behaviour as a function of temperature within the INC-phase. We believe that the formation of an ordered soliton structure below about 110 K is responsible for the considerably reduced damping of the phason mode. Even close to  $T_c$ , the lifetime of this mode is too small to allow to travel the distance between adjacent discommensurations. Hence, lattice dynamics within the soliton regime is entirely determined by the interactions within the commensurate domains. This conclusion is supported by the fact that no changes of the phase mode could be detected for applied fields of up to  $8\text{ kV cm}^{-1}$  as easily recognized by inspection of figure 10 (bottom). Obviously, the applied field does not change the structure and the polarization within the commensurate domains. Rather, the field acts only on the discommensurations that are displaced thus increasing the volumes of domains with parallel polarization.

NMR-experiments by Häcker *et al* [28] on  $\text{Rb}_2\text{ZnCl}_4$  have shown that the dynamics of nuclei located within the discommensurations is significantly different from those well within the commensurate domains. DC-fluctuations are softer than internal domain-fluctuations and the corresponding spin lattice relaxation rates differ by more than an order of magnitude. Moreover, the internal DC-relaxation rate increases on approaching  $T_c$  while the opposite behaviour is found for the domain relaxation. The present results for the lattice dynamics in  $\text{K}_2\text{SeO}_4$ , in particular the temperature dependent damping of the phase mode, correspond nicely to this view of reduced internal fluctuations close to  $T_c$  due to the formation of large commensurate domains separated by narrow discommensurations.

## 4. Discussion

In the soliton regime close to the lock-in transition, the INC-phase is usually regarded as an ordered sequence of commensurate domains that differ in the phase of the order parameter. In  $\text{K}_2\text{SeO}_4$ , the domain walls or discommensurations always separate domains of antiparallel electric polarization. The balance between attractive and repulsive interactions of neighbouring DCs leads to an almost regular domain pattern [48]. An applied electric field will

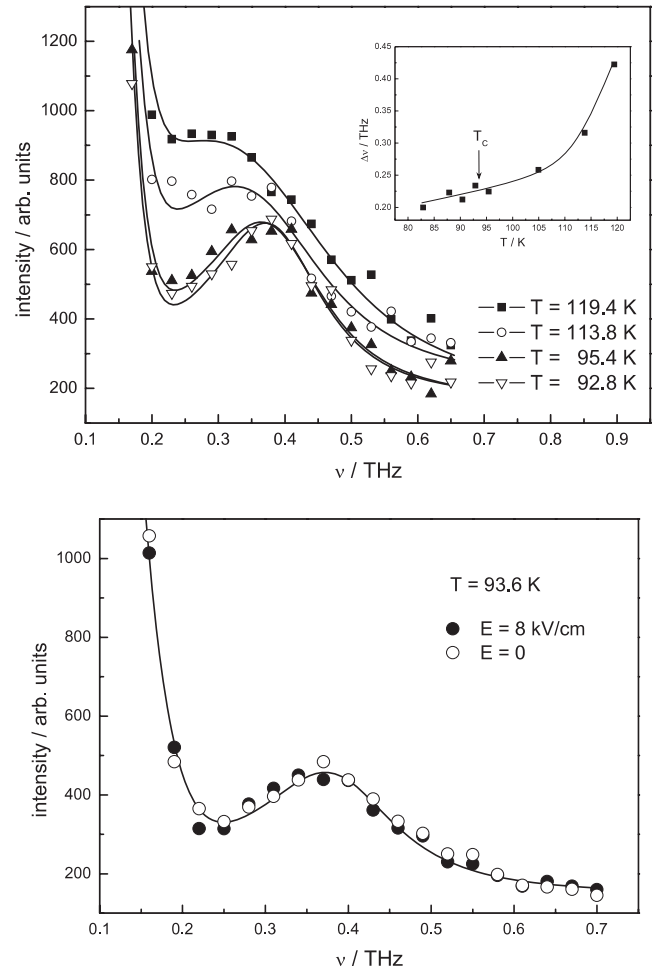


**Figure 10.** Top: temperature dependence of the phase mode spectrum at  $\mathbf{Q} = (4\ 0\ 1.2)$ . Note that the lowest temperature corresponds to the commensurate phase ( $T_c = 93.2\text{ K}$ ). The lines are the results of fits by damped harmonic oscillator functions superimposed on the elastic line. The inset shows the variation of the phonon line width  $\Delta\nu$ . Bottom: phase mode at  $T = 93.6\text{ K}$  and different applied electric fields.

favour each second domain of parallel polarization that grows in volume on the expense of the domains in between. If we assume that the applied electric field does not change the spontaneous polarization  $P_s$  ( $4.8 \times 10^{-8}\text{ C cm}^{-2}$  [7]) within the domains but merely moves the DCs, we are able to estimate the relative volume difference between neighbouring domains  $\Delta V/V$  and the ‘DC-relocatability’  $\Delta x/\Delta E$  (i.e. the field induced displacement) with the help of the following equations:

$$\frac{\Delta V}{V} = \frac{V_{\uparrow} - V_{\downarrow}}{V_{\uparrow} + V_{\downarrow}} = \frac{\Delta P}{P_s} = \frac{\varepsilon_0 \Delta \varepsilon}{P_s} \Delta E = 2 \Delta x \cdot \rho_{\text{DC}} \quad (11)$$

and

$$\frac{\Delta x}{\Delta E} = \frac{\varepsilon_0 \Delta \varepsilon}{2 \rho_{\text{DC}} P_s}, \quad (12)$$

$\Delta P$  and  $\varepsilon_0$  being the field induced polarization and the vacuum permittivity, respectively.

The latter quantity strongly increases on cooling as shown in figure 11 for zero field and  $E = 6.5\text{ kV cm}^{-1}$ . The

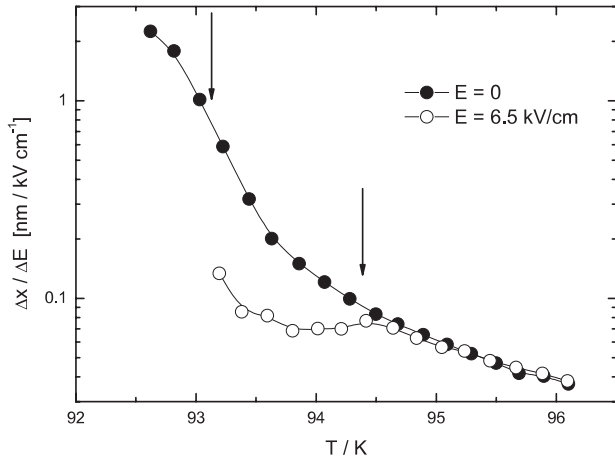


**Figure 11.** Temperature dependence of the field induced displacement of discommensurations. The arrows indicate the transition temperatures  $T_{\text{onset}}$  into the intermediate phase for  $E = 0$  and  $6.5 \text{ kV cm}^{-1}$ , respectively.

arrows indicate the transition temperatures from the INC to the intermediate phase at  $T_{\text{onset}}$ . Obviously, the ‘DC-relocatability’  $\Delta x/\Delta E$  is independent of the applied field as long as the homogeneous incommensurate phase is considered. At  $94.4 \text{ K}$  and  $E = 6.5 \text{ kV cm}^{-1}$ , the onset of the phase transition, the absolute DC-displacement reaches a value of about  $\Delta x \approx 0.46 \text{ nm}$  and part of the crystal becomes commensurate while the rest enters the intermediate diffuse phase.

This magnitude seems to be a characteristic quantity for the onset of the phase transition, since comparable values are obtained for different applied fields. This finding indicates that the well defined soliton lattice of the INC-phase with a characteristic DC-distance of about  $28 \text{ nm}$  (see above) becomes unstable as soon as the field induced volume difference of neighbouring domains with antiparallel polarization reaches a critical value of about  $3\%$ .

The quantity ‘DC-relocatability’ is closely related to the fluctuations of DCs. In  $\text{Rb}_2\text{ZnCl}_4$ , it is known from NMR-experiments that there is, in fact, a considerable softening of the DC-fluctuations on approaching the lock-in transition [28]. Hence, the present results are in perfect agreement with the concept of a soft soliton lattice close to the lock-in transition.

In order to get an idea about the properties of the intermediate phase let us assume that the contribution of the commensurate phase to the dielectric permittivity can be neglected and, hence,  $\Delta \varepsilon$  is entirely due to the motion of the DCs. Inspection of figures 7 and 8 yields that both, the permittivity and the misfit parameter (DC-density) decrease on cooling within the intermediate phase. As a result, the ‘DC-relocatability’ is no longer increasing but remains at about  $0.07 \text{ nm kV}^{-1} \text{ cm}^{-1}$  as shown in figure 11 which is about one order of magnitude smaller than in the zero field incommensurate phase. This result may be regarded as a direct experimental proof for the pinning of discommensurations within the intermediate phase. The combination of dielectric experiments and high-resolution diffraction allows us to obtain a quantitative characterization of pinning effects in modulated ferroelectrics.

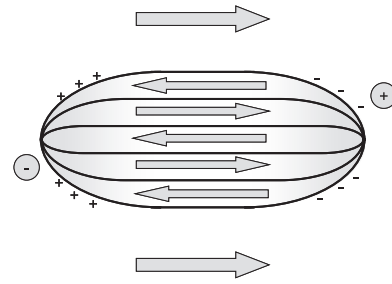


**Figure 12.** Isolated incommensurate nano-region within a commensurate ferroelectric domain.

A possible pinning mechanism leading to the formation of the disordered intermediate phase is based on the residual discommensurations that are unable to form complete stripples or antistripples as described in [33]. This view is in agreement with the increased width of the satellites as shown in figure 8 and the reduced coherence length of the modulation. Even the formation of isolated incommensurate regions is possible if the transverse motion of stripples or antistripples is hampered by some defects as depicted in figure 12. Since INC-phases are always the results of a competition between two or more order parameters, the discommensurations in  $\text{K}_2\text{SeO}_4$  are sources of mechanical strains [33, 44]. Moreover, it is well known [49] that non-planar parts of DCs carry a charge density. Hence, ionic defects that become mobile under the influence of an applied electric field are likely to be attracted by these regions, thus leading to a neutralization the surface charges. As an affect, the local electric field within these regions is shielded and they are stabilized until the lock-in temperature  $T_c$  for  $E = 0$  is reached.

Note, that the charge density needed to neutralize the surface polarization is less than one elementary charge per 500 elementary cells on the boundary. As a consequence, even extremely small defect concentrations can act as very efficient pinning centres.

The structure of the field induced intermediate phase of  $\text{K}_2\text{SeO}_4$  may tentatively be regarded as being complementary to the structure of relaxor ferroelectrics close to the diffuse phase transition. It is commonly accepted that *polar* nano-regions are responsible for the extraordinary properties of relaxors [50]. Our experimental findings in the modulated systems of  $\text{A}_2\text{BX}_4$ -compounds indicate that the unusual field induced behaviour is due to the presence of residual antiparallel domains. These are forming non-polar nano-regions within the polar commensurate surrounding. While the diffuse phase transition in relaxors becomes an ordinary ferroelectric transition under the influence of an applied field, the opposite behaviour is observed in the modulated systems like  $\text{K}_2\text{SeO}_4$  or  $\text{Rb}_2\text{ZnCl}_4$ : here, the first order transition in zero field gains a diffuse character under sufficiently large fields.

## 5. Conclusion

The combination of high-resolution  $\gamma$ -diffraction, elastic and inelastic neutron scattering as well as dielectric measurements

revealed an intermediate phase between the INC- and C-phase under the influence of an electric field. This phase is characterized by the appearance of pinned discommensurations and is similar to that found in the isostructural  $\text{Rb}_2\text{ZnCl}_4$ . It seems to be a general true equilibrium property of modulated ferroelectrics of the  $\text{A}_2\text{BX}_4$  group, irrespective whether the lock-in transition is of the displacive type like in  $\text{K}_2\text{SeO}_4$  or of the order–disorder type like in  $\text{Rb}_2\text{ZnCl}_4$ .

## Acknowledgment

This project was supported by the DFG under the grant number EC153/2-2.

## References

- [1] Cummins H Z 1990 *Phys. Rep.* **185** 211
- [2] Iizumi M, Axe J D, Shirane G and Shimaoka K 1977 *Phys. Rev. B* **15** 4392
- [3] Axe J D, Iizumi M and Shirane G 1980 *Phys. Rev. B* **22** 3408
- [4] Currat R and Janssen T 1988 *Solid State Phys.* **41** 201
- [5] Wada M, Uwe H, Sawada A, Ishibashi Y, Takagi Y and Sakudo T 1977 *J. Phys. Soc. Japan* **43** 544
- [6] Unruh H G, Eller W and Kirf G 1979 *Phys. Status Solidi a* **173** 435
- [7] Aiki K, Hukuda K, Koga H and Kobayashi T 1970 *J. Phys. Soc. Japan* **28** 389
- [8] Horioka M, Sawada A and Abe R 1981 *Ferroelectrics* **36** 347
- [9] Moudren A H, Moncton D E and Axe J D 1983 *Phys. Rev. Lett.* **51** 2390
- [10] Chaves M R, Almeida A, Tolédano J C, Schneck J, Kiat J M, Schwarz W, Ribeiro J L, Klöpperpieper A, Albers J and Müser H E 1993 *Phys. Rev. B* **48** 13318
- [11] Durand D, Dénoyer F and More M 1988 *Solid State Commun.* **66** 1195
- [12] Fousek J and Kroupa J 1988 *J. Phys. C: Solid State Phys.* **21** 5483
- [13] Strukov B A, Kobayashi J and Uesu Y 1985 *Ferroelectrics* **64** 57
- [14] Kroupa J, Ivanov N R, Fousek J and Chapelle J 1988 *Ferroelectrics* **79** 287
- [15] Elisbihani K and Eckold G 2004 *Ferroelectrics* **302** 115
- [16] McMillan W L 1976 *Phys. Rev. B* **4** 1496
- [17] Janovec V 1983 *Phys. Lett. A* **99** 384
- [18] Kawasaki K 1983 *J. Phys. C: Solid State Phys.* **16** 6911
- [19] Parlinski K 1987 *Phys. Rev. B* **35** 8680
- [20] Parlinski K, Dénoyer F and Eckold G 1991 *Phys. Rev. B* **43** 8411
- [21] Parlinski K 1988 *Comput. Phys. Rep.* **8** 153
- [22] Sakata H, Hamano K, Pan X and Unruh H G 1990 *J. Phys. Soc. Japan* **59** 1079
- [23] Aramburu I, Friese K, Pérez-Mato J M, Morgenroth W, Aroyo M, Brezowski T and Madariaga G 2006 *Phys. Rev. B* **73** 14112
- [24] Blinc R 1986 *Incommensurate Phases in Dielectrics* ed R Blinc and A P Levanyuk (Amsterdam: North-Holland) p 143
- [25] Pérez-Mato J M, Walisch R and Petersson J 1987 *Phys. Rev. B* **35** 6529
- [26] Topič B, Haeblerlen U and Blinc R 1990 *Phys. Rev. B* **42** 7790
- [27] Walisch R, Petersson J, Schüssler D, Häcker U, Michel D and Pérez-Mato J M 1994 *Phys. Rev. B* **50** 16192
- [28] Häcker U, Petersson J, Walisch R and Michel D 1996 *Z. Phys. B* **100** 441
- [29] Mischo P, Decker F, Holzer K-P, Petersson J, Häcker U and Michel D 1998 *J. Korean Phys. Soc.* **32** S873
- [30] Decker F, Häcker U, Holzer K-P, Irsch M, Michel D, Mischo P and Petersson J 2001 *Adv. Solid State Phys.* **41** 565
- [31] Chen C E, Schlesinger Y and Heeger A J 1981 *Phys. Rev. B* **24** 5139
- [32] Kudo S 1982 *Japan. J. Appl. Phys.* **21** 255
- [33] Eckold G, Hagen M and Steigenberger U 1998 *Phase Transit.* **67** 219
- [34] Hamano K, Ema K and Hirotsu S 1988 *Phase Transit.* **11** 279
- [35] Onodera A, Yamashita H and Molak A 1995 *Ferroelectrics* **172** 319
- [36] Gridnev S A, Gorbatenko V V and Prasolov B N 1995 *Ferroelectrics* **164** 349
- [37] Fousek J and Novotná V 1993 *Ferroelectrics* **140** 107
- [38] Majkrzak C F, Axe J D and Bruce A D 1980 *Phys. Rev. B* **22** 5278
- [39] Le Guillou J C and Zinn-Justin J 1977 *Phys. Rev. Lett.* **39** 95
- [40] Cowley R A and Bruce A D 1978 *J. Phys. C: Solid State Phys.* **11** 3577
- [41] Decker F, Häcker U, Holzer K-P, Mischo P, Petersson J and Michel D 1998 *Ferroelectrics* **208** 201 and references therein
- [42] Aslanyan T A 2004 *Phys. Rev. B* **70** 24102
- [43] Pérez-Mato J M, Gaztelua F, Madariaga G and Tello M J 1986 *J. Phys. C: Solid State Phys.* **19** 1923
- [44] Parlinski K and Dénoyer F 1985 *J. Phys. C: Solid State Phys.* **18** 293
- [45] Holakovský J and Dvořák V 1988 *J. Phys. C: Solid State Phys.* **21** 5449
- [46] Kobayashi J, Ozeki M, Kimura T, Tsutsumi Y, Tsukiji N, Shinbori E and Nakatsugawa H 1988 *Ferroelectr. Lett.* **8** 41
- [47] Quilichini M and Currat R 1983 *Solid State Commun.* **48** 1011
- [48] Levanyuk A P, Minyukov S A and Cano A 2002 *Phys. Rev. B* **66** 14111
- [49] Lajzerowicz J and Levanyuk A P 1994 *Ferroelectrics* **157** 63
- [50] Bokov A A and Ye Z G 2006 *J. Mater. Sci.* **41** 31